Defence Science Journal, Vol. 53, No. 1, January 2003, pp. 75-86

Finite-element Analysis of Composite Pressure Vessels with Progressive Degradation

Nagesh

Indian Institute of Technology Delhi, New Delhi–110 016

ABSTRACT

A degradation model incorporated into the finite-element analysis of the pressure vessel, based on a progressive failure criterion, has been discussed. A stiffness reduction scheme for the failed laminas has been implemented using package ANSYS along with a reduction in the strength of the composite (on its undegraded strength after a substantial degradation of its constituents). The degradation model used for analysis is sensitive to the mesh and the load step size. Computational efficiency (CPU time) of the finite-element model is very important in the degradation study, and accordingly, equilibrium is not re-established in the nonlinear solution procedure implemented in ANSYS (single-frame restart analysis). This is offset using a small load step size for the degradation studies of the pressure vessel.

The model is qualified by a comparison with deformation measurements obtained from hydrostatic tests. The experimental deformations have an excellent match with the degraded model in comparison to the undegraded model. The redistribution of stresses in the composite constituents as a result of degradation, has been demonstrated. The burst in the pressure vessel is indicated by unusually large displacement and infeasible stress profile in consequence to a substantial degradation in the fibre material of the composite.

Keywords: Finite-element analysis, composite pressure vessel, progressive degradation, degradation model, failure analysis

NOMENCLATURE

E_{xx}	Longitudinal modulus
E_{yy}	Transverse modulus
G_{xz}, G_{xy}, G_{yz}	Shear tangent moduli
ν_{xy}, ν_{yz}, ν_{xz}	Poisson's ratios
F_s	Unidirectional lamina shear strength
F_{1T}	Unidirectional lamina tensile strength in fibre direction
F_{2T}	Unidirectional lamina tensile strength in transverse direction
σ_{11}, σ_{22}, σ_{33}	Normal stress components in principal material axis system
σ_{12}, σ_{23}, σ_{13}	Shear stress components in principal material axis system

Received 24 October 2002

1. INTRODUCTION

Failure is addressed wrt that of a unidirectional lamina considering it as a part of a composite orthotropic laminate. Strength of a lamina is the basic aspect considered for the strength and failure analysis of a laminate. A composite laminate has many peculiarities. The strength of the lamina is directionally-dependent. The strength in tension and compression of a unidirectional composite differs significantly. The lamina failure criterion can be either with independent failure mode where the onset as well as the mode of failure can be predicted, or the interaction failure criterion where only the onset of failure is predicted.

Failure in a composite is initiated due to the following:

(a) Fibre-dominated failure (breakage, micro-buckling, dewetting)

(b) Bulk matrix-dominated failure (cracking, voids)

(c) Interface/flaw-dominated failure (crack propagation, edge delamination).

The failure of a lamina in a laminate, i.e., the first ply failure (FPF) does not necessarily signify failure of the structure, as the failure of fibre-reinforced plastic laminate is gradual and progressive. When a particular lamina fails in a laminate, a redistribution of stress takes place in the remaining lamina. The laminate can be considered failed when the maximum load level is reached following a multilayer failure, i.e. the ultimate laminate failure (ULF). It is therefore important to study the behaviour of the laminate after failure has occurred in a lamina until the laminate fails totally so that the load carrying capacity of the laminate is determined. This is termed as post-failure or progressive degradation analysis.

2. SOME POST-FAILURE THEORIES

Nahas[1] has presented a good overview of all available post-failure composite theories. The Hahn-Tsai method assumes that any failed lamina will support its load, which it was carrying when it failed, until total laminate failure occurs (Fig. 1). The problem is approached with linear analysis by replacing the Young's moduli and shear moduli of degraded layers with reduced values.

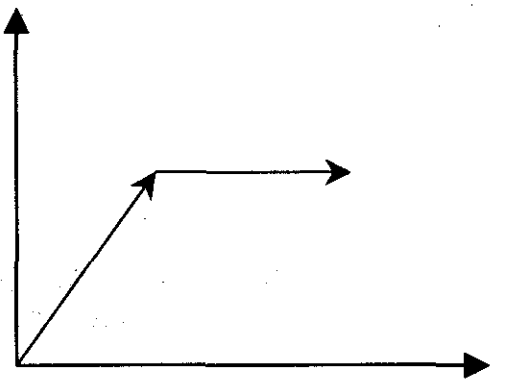

Figure 1. Failed lamina supports its load

In the Petit-Waddoups method, the failed lamina unloads gradually. Mathematically, this is done by giving the tangent modulus a relatively high negative value as shown in Fig. 2. The Chiu theory assumes that instantaneous unloading for the failed layers takes place as shown in Figure 3. Chiu determined the mode of failure by checking the strains in the individual layers and observed that the failed layers unload in the direction in which the failure had occurred. Nahas assumed that the failed layer unloads

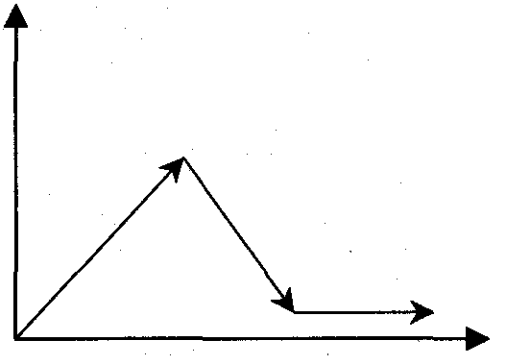

Figure 2. Failed lamina unloads gradually

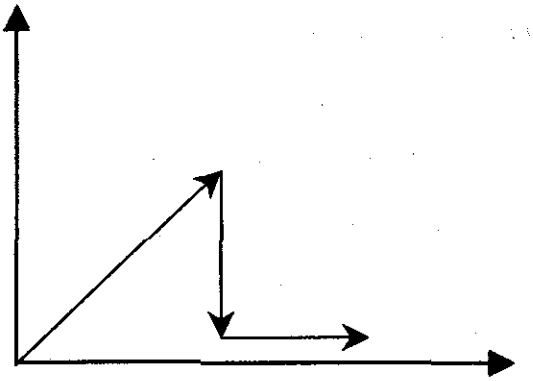

Figure 3. Failed lamina unloads drastically

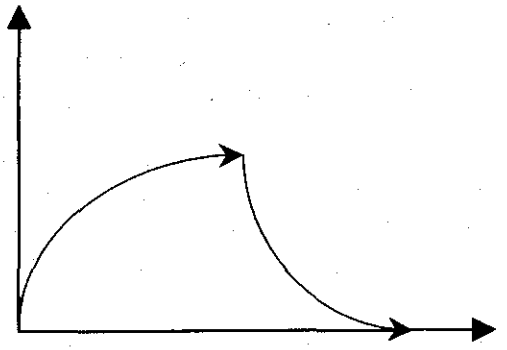

Figure 4. Nonlinear behaviour of lamina

gradually in the direction of the failure, following an exponential function as shown in Fig. 4.

3. COMPOSITE PRESSURE VESSEL S44

The specific vessel under investigation is called S44 (Fig 5) that forms the 4th stage rocket motor case of a satellite launcher. The motor case is manufactured using aramid fibres (Kevlar-49) and epoxy resin by means of wet filament winding and the motor case acts essentially as a pressure vessel. In the particular function as an Apogee motor for orbital missions, the total engine mass consists of a solid fuel, nozzle, and a pressure vessel mass which is included in the payload calculations. A minimisation of the vessel mass therefore clearly implies a bigger payload or a higher orbit.

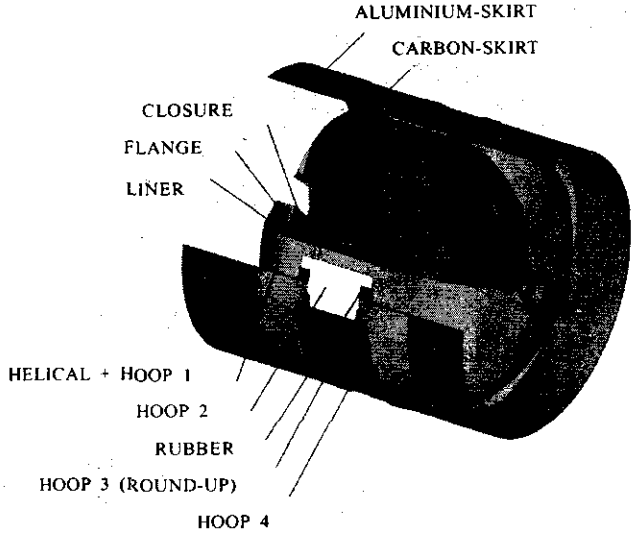

Figure 5. Composite pressure vessel S44

The first winding stage (filament winding technique) results in an alternate stack of five groups of hoop plies (on the cylindrical part only) and helical plies. Then, part of the outer hoop layers are applied followed by the mounting of the prefabricated skirts. The skirts are fixed in place with the hoop layers. The rubber liner inside the composite material is installed on the mandrel prior to winding and assures the pressure tightness in spite of matrix cracks.

4. LAMINATE LAY-UP

The lay-up for S44 in way of the cylindrical portion without hoop 3 is:

$$\left[(90^\circ \,|\, +\alpha \,|\, -\alpha)_5 \,|\, (90^\circ)_{14}\right]$$

The lay-up designation in way of hoop 3 is

$$\left[(90^\circ \,|\, +\alpha \,|\, -\alpha)_5 \,|\, (90^\circ)_{21}\right]$$

The lay-up designation in way of the domes is

$$\left[(90^\circ \,|\, +\alpha \,|\, -\alpha)_5\right]$$

The fibre material for the composite pressure vessel in dome and cylinder area is Kevlar-49 (Fig. 6). The vessel has a skirt made of carbon fibres, which is bolted to the aluminium part of the skirt through which the pressure vessel is attached to the vehicle for thrust transfer.

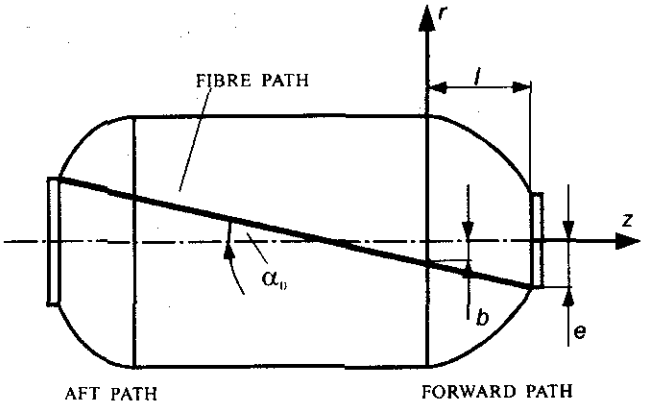

Figure 6. Fibre path for planar winding

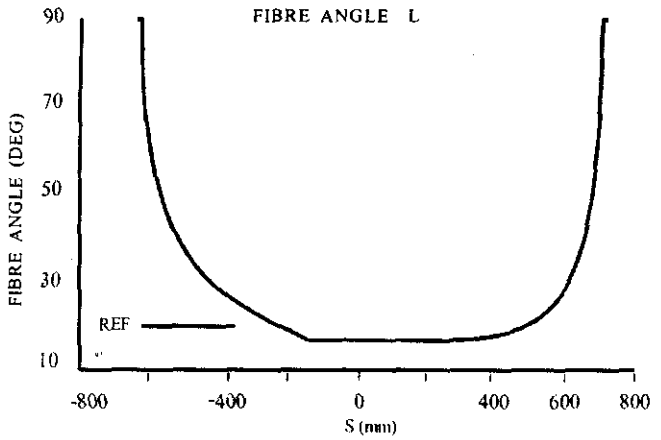

Figure 7. Winding angle on a contour path along a meridian cut for the complete vessel.

5. PRESSURE VESSEL GEOMETRY & FINITE ELEMENT MODEL IN ANSYS

The dome contour/geometry are determined according to netting theory, as discussed by Nagesh[2] and Loures[3]. This geometry is used as the winding surface and the slope at the inflection point is used to continue the contour to the opening as a straight line in the meridian cut. The winding angle distribution, depending on the dome contours and the cylinder length, is calculated and shown in Fig. 7. The incorporated wall thickness distribution is based on measurements. The dome contours together with the winding angle are stored in data tables. These are used to generate a solid geometry model within the finite-element analysis package ANSYS.

Krieger[4], *et al.* gave a detailed description of the concepts/methodology employed in the finite-element modelling of S44 in package ANSYS. An important feature of the modelling concept is that the finite-element mesh is flexibly created by an automated preprocessor on the basis of user-specified parameters. The parameters are defined by the geometry of the pressure vessel to be analysed and the mesh density of the desired finite-element model. The models for the present study have been created in three basic steps. In the first step, contour, winding angle, and thickness distributions of the pressure vessel are calculated on the basis of netting analysis equations for either planar or geodesic winding, and using theoretical or empirical models for the wall thickness distribution. These calculations depend on the user-specified parameters like diameter, length, and filament bandwidth. The results of this step are presented in data tables. In the second step, a solid geometry model of the pressure vessel is created based on the data tables from the first step and additional parameters selected by the user. This geometry model consists mainly of volume entities.

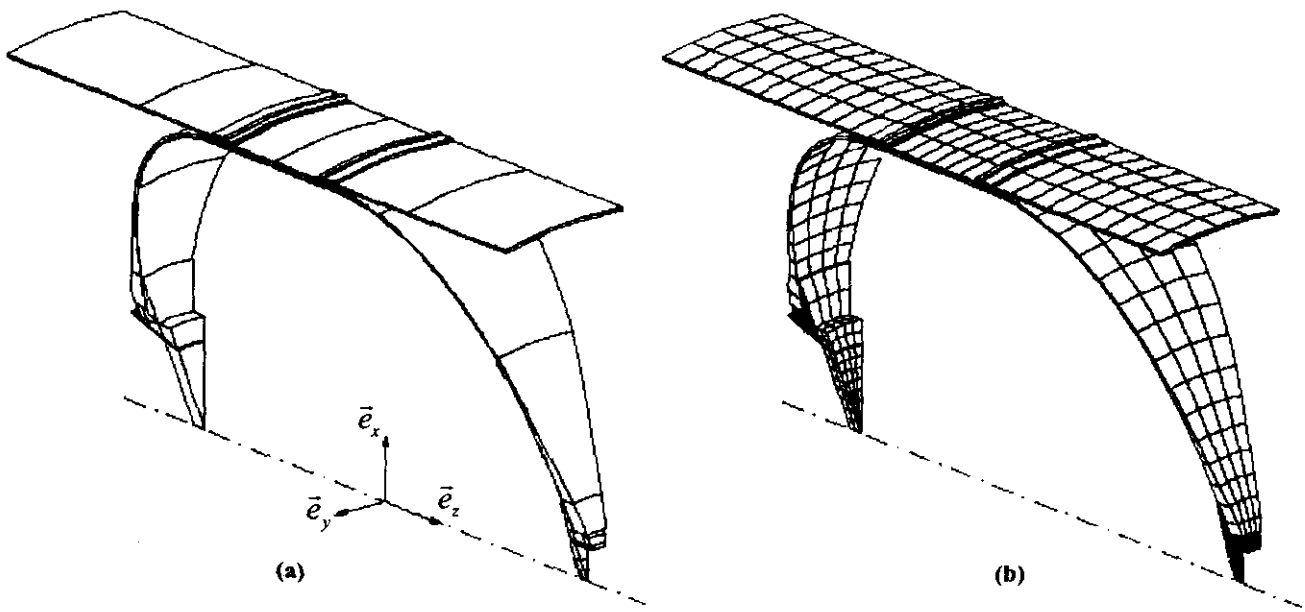

Figure 8. (a) Solid geometry model and (b) finite-element mesh (20° sector)

In the third step, the finite-element model consisting of structured meshes is created by mapped meshing. Structured meshes are the most appropriate for the selected layered volume elements. Mesh densities can be controlled by the user through the selection of parameters. While mesh densities in meridian and circumferential directions can be selected from a nearly-arbitrary range, this is currently not true in the thickness direction.

For the lay-up of the motor case, either one or five elements in thickness direction can be selected. Figure 8 shows a solid geometry model (a) and the associated finite-element model (b). In this case, a 20° sector model with four elements in circumferential and one element in thickness direction was created by the preprocessor. The thickness is flexible within each hoop production stage and can be adjusted in discrete steps. The length of the cylindrical part and the skirt lengths can be chosen. The wall thickness of the helical windings at the equator are also determined by the user. The nonlinear analysis is an option, but it is recommended due to the nonlinear geometrical behaviour of these vessels. Additional parameters are controlling further options of the widely parameterised model. The model can be built without skirts for either evaluating their influence or for the simulation of other pressure vessel types.

The finite-element sector model consists of only one element in the circumferential direction. The composite areas are represented by 8-node layered composite volume elements with transverse orthotropic material for each layer. The orthotropic material together with classical symmetry boundary conditions in terms of displacement constraints for sector models would lead to asymmetric stress distributions along the circumference. An axisymmetric solution is enforced for the present model using coupling conditions for the same degrees-of-freedom (DOFs) in cylindrical coordinates within each node row along the circumference. Multhoff[5], *et al.* describe the employed method. The method has been validated with the help of composite cylindrical models presented by Nagesh[2].

After the numerical simulation is done, the postprocessing is performed in a special way. For all the composite plies, evaluation paths along the surfaces of the contour are created and the results are transformed pointwise into local coordinate systems. These results are recorded for the helical and the hoop windings along a meridian. For the stress evaluation of the helical plies, it is important to have inside, midplane and outside paths to determine and visualise the bending and membrane part of the stress as shown in Fig. 9.

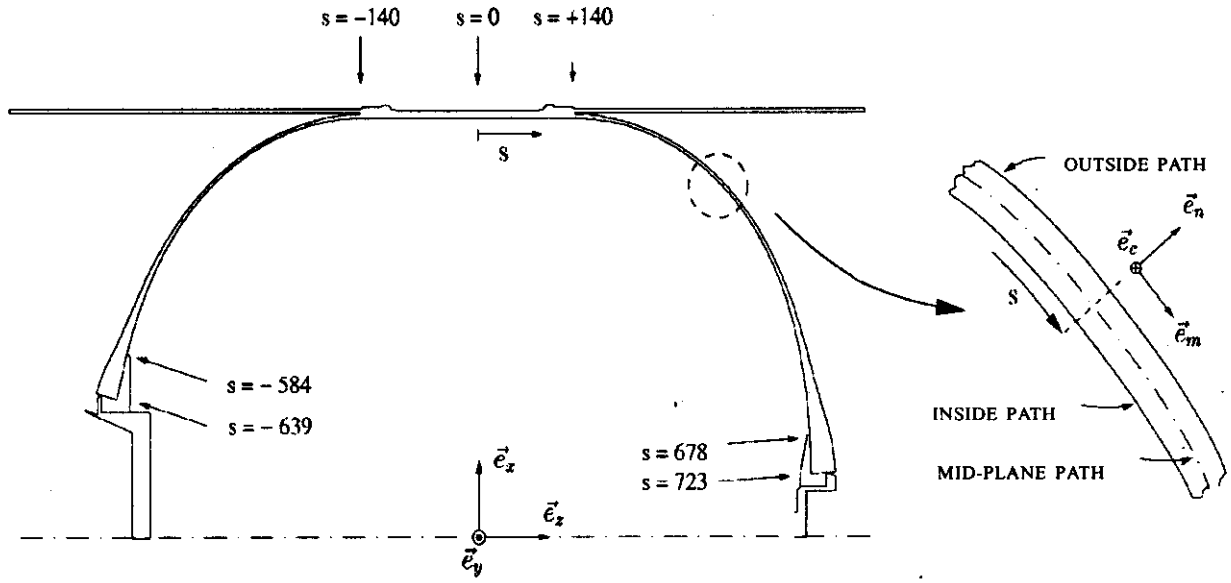

Figure 9. Edge plot of meridian cut of the finite-element model

6. PROGRESSIVE FAILURE ANALYSIS

The finite-element method is useful to analyse the fibre composite structure in the progressive failure analysis. Chang[6] has developed a failure criterion in conjunction with analysis of the nonlinear behaviour of composite material and property degradation model using the fibre bundle theory. A progressive failure technique building upon the idea suggested by Chang[6], Doh[7], *et al.* and Sleight[8], *et al.* is incorporated in the nonlinear analysis.

To identify the damage zone of the filament wound pressure vessel, three types of damages are considered. These are: (i) matrix tensile failure, (ii) fibre breakage failure, and (iii) fibre-matrix shear failure.

6.1 Matrix Tensile Failure ($\sigma_{22} \geq 0$)

For predicting matrix cracking the criterion has the following form:

$$\left[\frac{\sigma_{22}}{F_{2T}}\right]^2 + \left[\frac{\sigma_{23}}{F_s}\right]^2 + \left[\frac{\sigma_{12}}{F_s}\right]^2 + \left[\frac{\sigma_{13}}{F_s}\right]^2 = I_m \qquad (1)$$

6.2 Fibre & Fibre-matrix Shearing Failure ($\sigma_{11} \geq 0$)

For predicting the fibre breakage or fibre-matrix shearing failure, the criterion has the following form:

$$\left[\frac{\sigma_{11}}{F_{1T}}\right]^2 + \left[\frac{\sigma_{12}}{F_s}\right]^2 + \left[\frac{\sigma_{13}}{F_s}\right]^2 = I_f \qquad (2)$$

The fibre breakage-dominated failure occurs when

$$\left[\frac{\sigma_{11}}{F_{1T}}\right]^2 \geq \left[\frac{\sigma_{12}}{F_s}\right]^2 + \left[\frac{\sigma_{13}}{F_s}\right]^2 \qquad (3)$$

otherwise, the fibre matrix shearing-dominated failure occurs:

$$\left[\frac{\sigma_{11}}{F_{1T}}\right]^2 < \left[\frac{\sigma_{12}}{F_s}\right]^2 + \left[\frac{\sigma_{13}}{F_s}\right]^2 \qquad (4)$$

6.3 Property Degradation Model

Once the failure occurs (*i.e.*, I_m or $I_f \geq 1$), the degradation of mechanical properties depends on the type of failure mode, which is predicted as follows:

6.3.1 *Matrix Failure*

For the matrix-cracking failure in a layer, the transverse modulus E_{yy}, Poisson's ration ν_{xy}, and the shear modulus G_{yz} should be reduced to zero. The longitudinal modulus E_{xx}, and the shear tangent modulus G_{xy}, and G_{xz} are unchanged in the failed layer of an element. The material properties of the damaged layers considering the stability of the stiffness matrix in ANSYS are modified as

E_{xx}: Same	G_{xy}: Same	ν_{xy}: 0
E_{yy}: 90 % degraded	G_{yz}: 90 % degraded	ν_{yz}: Same
E_{zz}: 90 % degraded	G_{xz}: Same	ν_{xz}: 0

6.3.2 *Fibre Breakage & Fibre-matrix Shearing Failure*

For the element damage with the fibre breakage criterion, Poisson's ratio ν_{xy}, and transverse modulus E_{yy}, are reduced to zero and the longitudinal modulus E_{xx} and the shear modulus G_{xy} and G_{xz}, degenerated. Considering the stability of stiffness matrix of the material in ANSYS, the properties are degraded to 90 per cent of their original values. The modified material properties are as follows:

E_{xx}: 90 % degraded	G_{xy}: 90 % degraded	ν_{xy}: 0
E_{yy}: 90 % degraded	G_{yz}: 90 % degraded	ν_{yz}: Same
E_{zz}: 90 % degraded	G_{xz}: 90 % degraded	ν_{xz}: Same

For the fibre-matrix shearing-dominated failure, the material properties for the failed elements are degenerated/modified as follows:

manifest as a non-convergence of the nonlinear solution at that load step.

However, the iterative solution to re-establish equilibrium of the structure at each load step post-material model modification, is computationally very expensive. Hence to bring the computation time within feasible limits, presently equilibrium is not re-established in the nonlinear solution procedure implemented in ANSYS (single-frame restart analysis). To make up for this, the strategy has been to use small load increments, which minimise the effect of not re-establishing equilibrium as shown in Fig. 10. The computer program that carries out this degradation solution procedure in ANSYS has been elaborated by Nagesh[2]. The numerical procedures for the proposed analysis are performed in the following five steps:

Step 1. Increase the applied load from P^n to P^{n+1} by small increment ΔP in the solution processor.

Step 2. Check for the element state of stress after the load step nonlinear analysis in the postprocessor and evaluate the failure indices and damage criteria, i.e., I_m and I_f.

Step 3. If no failure occurs, proceed to the next load step.

Step 4. If failure occurs (i.e., I_m or $I_f \geq 1$), then effect a suitable modification to the element material property pointer (real constant set). For the next load step, the modified material properties are used. The next step is started from the end of the last damage stabilisation load step using a single-frame restart using the modified/degraded material properties of the elements.

Step 5. Degrade the composite tensile and shear strength properties by a suitable margin once the matrix and associated degradation has taken place.

8. RESULTS & CONCLUSIONS

Figures 11 and 12 show a comparison of the normal displacements along the outside meridian path of the process vessel for the finite-element

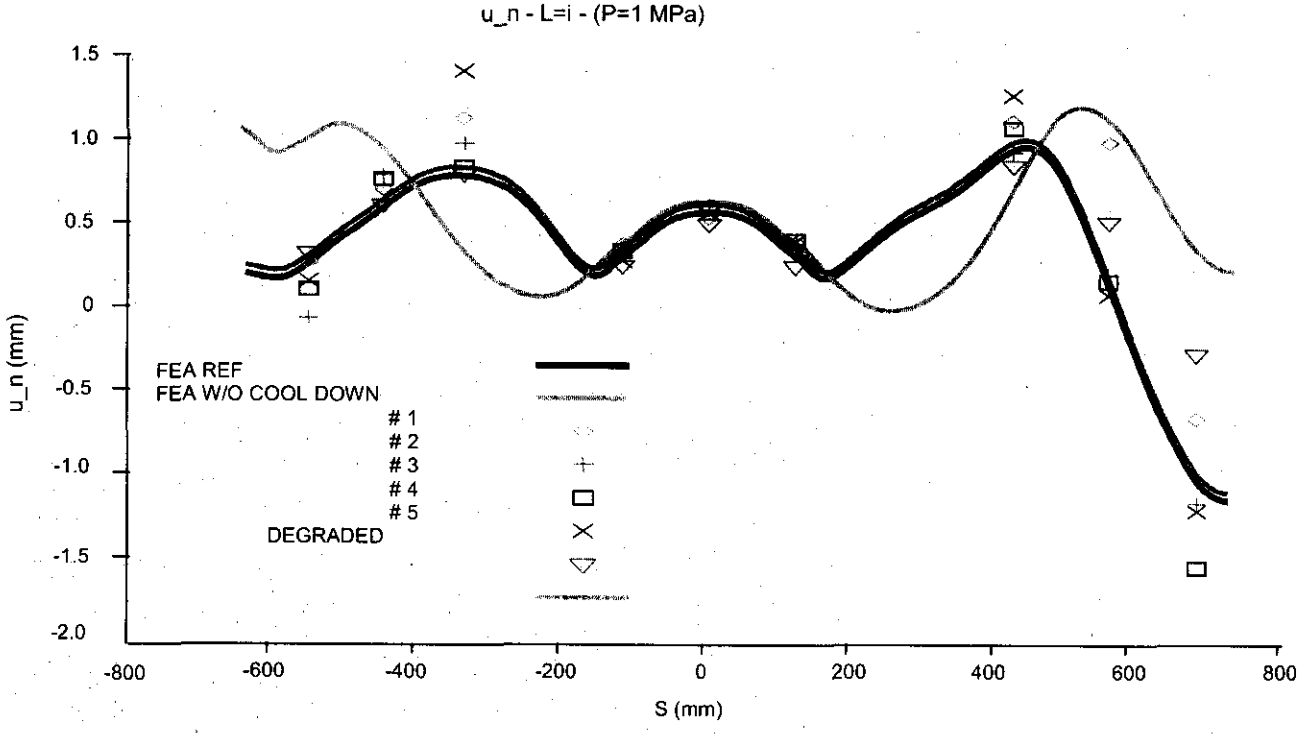

Figure 11. Normal displacement along outside meridian path. Experimental results compared with finite-element analysis reference model with and without degradation and model without cool down analysis at 1 MPa.

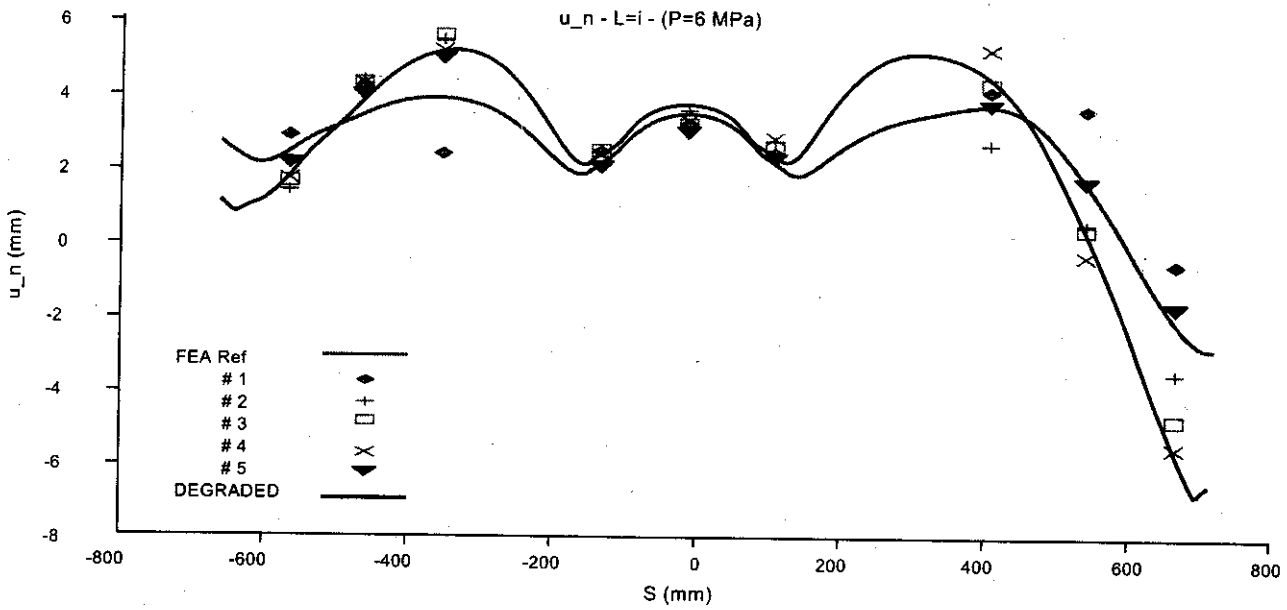

Figure 12. Normal displacement along outside meridian path. Experimental results compared with finite-element analysis reference model without degradation and degradation model at 6 MPa.

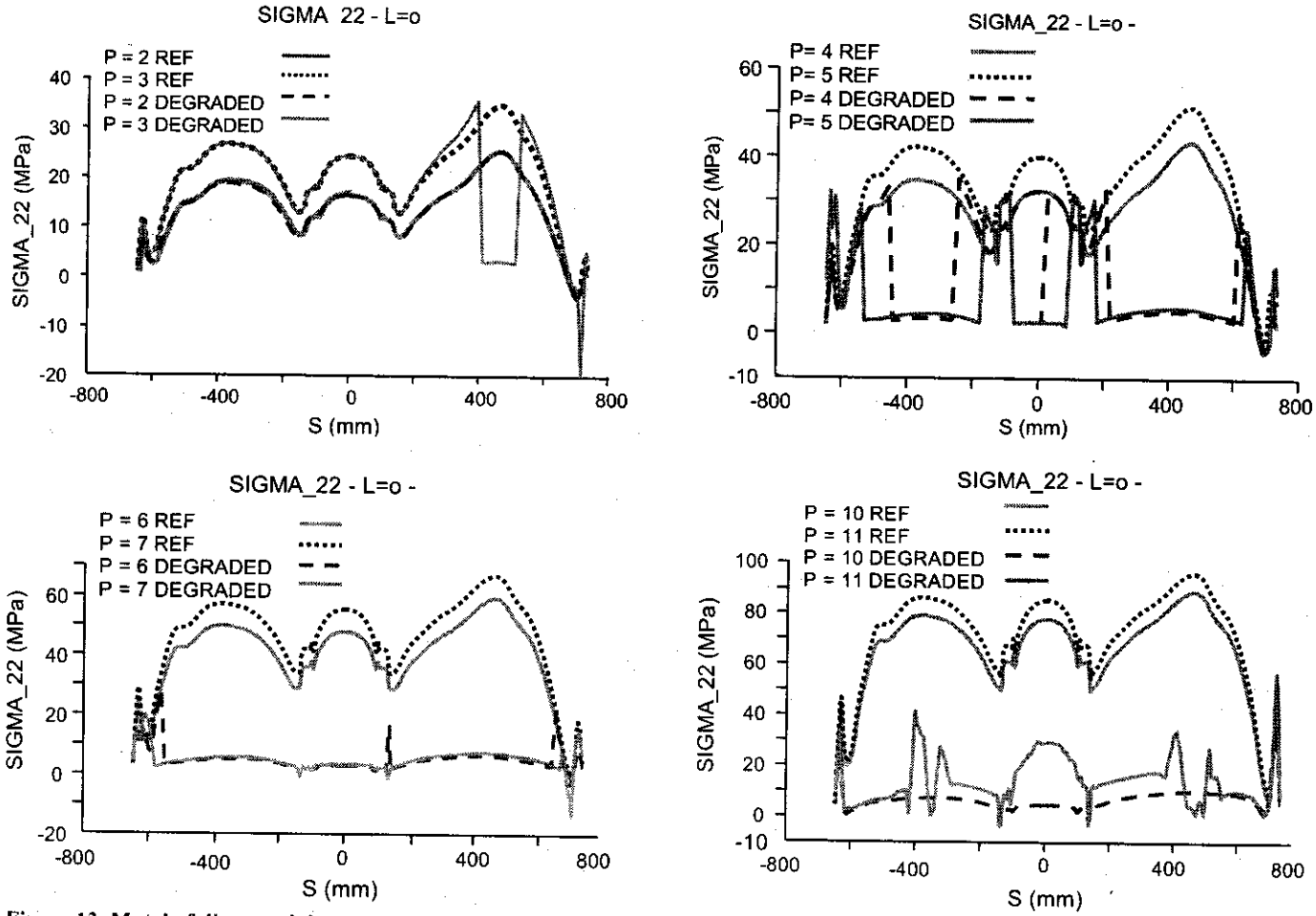

Figure 13. Matrix failure and damage propagation. Stress in matrix direction at various pressure levels for finite-element analysis reference model versus degradation model.

experimental hydrostatic test measurements. Since no damage in composite constituents is initiated at 1 MPa, both the finite-element analysis reference model and the degradation model results coincide. It is important to include the cool down deformations in the pressure vessels without which the comparison of normal displacements is quite poor. Failure initiation takes place in the form of matrix-cracking in a few elements and gradually spreads to other elements with the increase in loading. As the matrix fails in an element, a redistribution of stresses in the adjacent elements takes place, which manifests as a visible increase in the fibre direction stresses and displacement response, especially in the region of cracked matrix.

The propagation of damage in the matrix, from initiation at 3 MPa at the forward dome has been demonstrated in Fig. 13. As the pressure level reaches 4 MPa, the matrix damage zone grows in the forward dome and matrix damage is initiated at the aft dome as well. Notice the increased stress levels in the zone adjacent to the failed one due to redistribution. As the pressure level further increases, the matrix damage zone further grows and by 6 MPa, almost the whole matrix in the pressure vessel is cracked. This is indicated by dropped stress levels in the

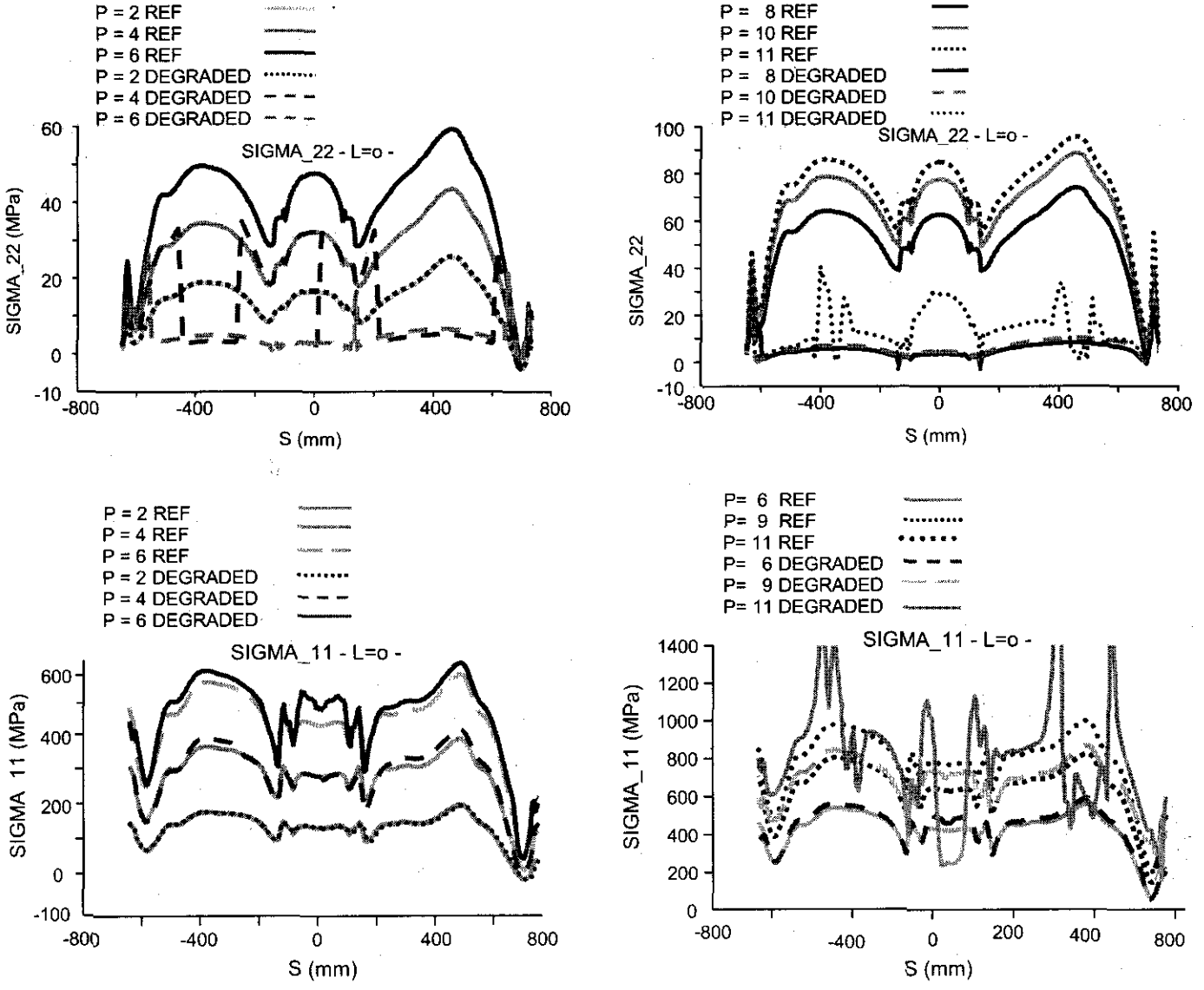

Figure 14. Failure, damage propagation, and burst. Stresses in matrix and fibre direction for finite-element analysis reference model versus degradation model. Burst indicated by an uncharacteristic stress profile in fibre as well as matrix direction.

This is indicated by dropped stress levels in the matrix direction and a corresponding increase in the fibre direction stress as seen in Fig. 13 when compared with the undegraded finite-element analysis reference models. The degradation model caters for a reduction in the composite strength post-extensive failure of matrix, in addition to the failed element stiffness modifications at each load step in the proposed degradation model.

Figure 14 shows the propagation of damage in matrix and fibres of the composite with increasing load levels, from initiation of matrix-cracking at 3 MPa to burst of matrix at 11 MPa. The bursting condition is reached with the failure of a significant number of fibres between 10.5 MPa and 11 MPa indicated by a physically infeasible stress profile (beyond the material strength) and an uncharacteristic displacement profile. The reduced stress levels are noticed in the cracked matrix showing an abrupt increase due to extensive fibre failure (breakage) at 11 MPa. This finite-element analysis-predicted burst pressure between 10.5 MPa and 11 MPa is in good agreement with the mean burst pressure of 10.59 MPa from the hydroburst pressure tests. The model is qualified after comparisons of normal displacement along the meridian path from the hydrostatic tests and the finite-element analysis reference model with and without degradation. It is evident from Fig. 12 that the plotted normal displacement results of degradation have an excellent fit with the experimental data in comparison to the undegraded finite-element analysis reference model.

REFERENCES

1. Nahas, M.N. Survey of failure and post-failure theories of laminated fibre reinforced composites. *J. Composite Tech. Res.*, 1986, **8**(4), 138-53.
2. Nagesh, Finite-element analysis of composite pressure vessels under multiple load cases. PhD Thesis, 2002, Indian Institute of Technology, Kharagpur, India/RWTH Aachen, Germany.
3. Loures da Costa, L.E.V.; Multhoff, J.B.; Krieger, J. & Betten, J. Structural development of the S33 rocket motor case. (Proceedings of COBEM 2001). *Aerospace Engineering*, 2001, **6**, 237-46.
4. Krieger, J.; Multhoff, J.B.; Loures da Costa, L.E.V. & Betten, J. Development of a finite-element model for composite pressure vessels and its application in structural optimisation. (Proceedings of COBEM 2001). *Aerospace Engineering*, 2001, **6**,360-75.
5. Multhoff, J.B.; Krieger, J.; Loures da Costa, L.E.V. & Betten, J. Problems on high-resolution finite-element models of composite rocket motor cases. (Proceedings of COBEM 2001). *Aerospace Engineering*, 2001, **6**, 207-16.
6. Chang, F.K. A progressive design models for laminated composites containing stress concentrations. *J. Compos. Mater.*, 1987, **21**, 832-55.
7. Doh, Y.D. & Hong, C.S. Progressive failure analysis for filament wound pressure vessel, *J. Reinforced-Plastics Compos.*, 1995, **14**, 1278-306.
8. Sleight, D.W.; Knight, N.F. & Wang, J.T. Evaluation of a progressive failure analysis methodology for laminated composite structures. 38th Structures, Structural Dynamics and Materials Conference, 1997. AIAA Paper No. 97-1187.